

# van der Waals clusters of pyridazine and isoquinoline: The effect of solvation on chromophore electronic structure

J. Wanna and E. R. Bernstein

Citation: *The Journal of Chemical Physics* **86**, 6707 (1987); doi: 10.1063/1.452369

View online: <http://dx.doi.org/10.1063/1.452369>

View Table of Contents: <http://aip.scitation.org/toc/jcp/86/12>

Published by the *American Institute of Physics*

---

---



**COMPLETELY  
REDESIGNED!**

**PHYSICS  
TODAY**

*Physics Today* Buyer's Guide  
Search with a purpose.

# van der Waals clusters of pyridazine and isoquinoline: The effect of solvation on chromophore electronic structure<sup>a)</sup>

J. Wanna and E. R. Bernstein

Department of Chemistry, Condensed Matter Sciences Laboratory, Colorado State University, Fort Collins, Colorado 80523

(Received 16 December 1986; accepted 6 March 1987)

van der Waals clusters of pyridazine and isoquinoline with CH<sub>4</sub>, NH<sub>3</sub>, H<sub>2</sub>O, and CH<sub>3</sub>OH are generated in a supersonic molecular jet expansion and investigated by two-color time-of-flight mass spectroscopy. As is the case for the other diazine systems, no spectra could be observed for pyridazine (H<sub>2</sub>O)<sub>n</sub> or (CH<sub>3</sub>OH)<sub>n</sub> clusters. Both chromophore molecules are reported to have close lying, vibronically coupled S<sub>1</sub> and S<sub>2</sub> excited states: nπ\* for pyridazine and nπ\* (S<sub>1</sub>) and ππ\* (S<sub>2</sub>) for isoquinoline. Cluster spectra for pyridazine methane and ammonia clusters do not favor the presence of two nπ\* transitions in the S<sub>1</sub> ← S<sub>0</sub> transition region but rather suggest that the "S<sub>2</sub> origin" is a vibronic feature of the S<sub>1</sub> ← S<sub>0</sub> transition. Isoquinoline clusters that are only weakly or not at all hydrogen bonded (CH<sub>4</sub> and NH<sub>3</sub>) display a complicated spectrum indicative of S<sub>1</sub> (nπ\*)–S<sub>2</sub> (ππ\*) vibronic coupling and not the usual shifted isolated molecular spectrum. Isoquinoline clusters with substantial hydrogen bonding (H<sub>2</sub>O and CH<sub>3</sub>OH) display relatively simple spectra indicative of only a single electronic transition S<sub>2</sub> (ππ\*) ← S<sub>0</sub> in the region and no interstate vibronic coupling. These results are compared and contrasted with each other and the spectra of the other diazine clusters. Potential energy calculations are also employed to help understand the clustering in these systems.

## I. INTRODUCTION

van der Waals clusters generated in a supersonic molecular jet expansion provide a novel means of studying the detailed nature of intra- and intermolecular interactions in systems for which two electronic states are vibronically coupled. The affect of solvation on each electronic state can be quite different, thus allowing one to separate the two states and evaluate the extent of and the mechanisms of the vibronic interactions in the clustered chromophore. In addition, two excited electronic states are accessible in such systems and both can be employed to probe the cluster solute (chromophore)/solvent intermolecular interactions. In these studies, one can assess the affect of weak and strong hydrogen bonding solvents on chromophore nπ\* and ππ\* excited electronic states and their interaction. A number of different cluster systems have been studied for both nπ\* and ππ\* electronic states with solvents of various hydrogen bonding strengths.<sup>1-5</sup>

Clusters of pyridazine and isoquinoline with various alkanes and hydrogen bonding solvents are discussed in this paper. Pyridazine and isoquinoline are interesting chromophores because they are reported to have two nearly isoenergetic low lying singlet excited electronic states (both nπ\* for pyridazine and nπ\* and ππ\* for isoquinoline) accessible for optical spectroscopy. In addition, pyridazine fills out our study of diazine/solvent systems.<sup>4,5</sup>

The low lying excited singlet electronic states of pyridazine have not been definitively assigned as yet. An nπ\* origin is assigned at 26 649 cm<sup>-1</sup>; 373 cm<sup>-1</sup> to higher energy is a

feature that, based on rotational analysis<sup>6</sup> and solvent matrix effects,<sup>7</sup> has been assigned as a new nπ\* electronic origin. Theoretical calculations<sup>8</sup> do not support this contention, however. The S<sub>2</sub> state is predicted to be higher than S<sub>1</sub> by more than 20 000 cm<sup>-1</sup>. Other candidates for the S<sub>1</sub> + 373 cm<sup>-1</sup> feature in the pyridazine spectrum include 10a<sub>0</sub><sup>1</sup>, 16a<sub>0</sub><sup>2</sup>, 16b<sub>0</sub><sup>2</sup>, and 6a<sub>0</sub><sup>1</sup>.

Clusters of pyridazine with methane and ammonia are presented here in comparison with similar pyrazine and pyrimidine clusters. In addition, the 373 cm<sup>-1</sup> feature can be studied in the clusters: if this is the S<sub>2</sub> (nπ\*) origin, one might expect different shifts and van der Waals (vdW) vibrational modes than found for the S<sub>1</sub> (nπ\*) origin. The vibrational modes of the pyridazine (NH<sub>3</sub>)<sub>1</sub> cluster can be analyzed utilizing an intermolecular normal coordinate analysis.<sup>9</sup> Pyridazine water and methanol clusters could not be observed: a similar situation arose for the other diazine systems.<sup>5,10</sup>

The assignments for the excited electronic states of isoquinoline seem much more certain. Isoquinoline has a weak S<sub>1</sub> (nπ\*) transition whose origin is at 30 821 cm<sup>-1</sup>.<sup>11</sup> The S<sub>2</sub> state is identified as ππ\* with its origin at 31 929 cm<sup>-1</sup>. This feature is one of three intense bands in the region. The other intense features are suggested to arise from the near resonance vibronic coupling of two S<sub>1</sub> (nπ\*) vibronic states with the S<sub>2</sub> (ππ\*) origin. Isoquinoline clusters with methane, ammonia, methanol, and water are reported and analyzed in this paper. The changes in vibronic coupling in this region due to the clustering interactions are discussed. Clusters have a large effect on the nπ\*–ππ\* state vibronic interactions because of solvent effects on the relative positions of S<sub>1</sub> and S<sub>2</sub>.

<sup>a)</sup> Supported in part by a grant from ONR.

Intermolecular potential energy calculations, utilizing an additive atom-atom potential in a Lennard-Jones (LJ) format, are performed to obtain cluster ground state binding energy, geometry, and intermolecular motion. A (10-12) potential form is used to model atom-atom hydrogen bonding, a (6-12) form is used to model other nonbonded dispersion interactions, and a single Coulomb term is employed for the partial atomic charge contribution to the cluster interaction. Thus the overall atom-atom potential forms for dispersion and hydrogen bonding are (6-12-1) and (10-12-1), respectively. The LJ parameters used in this calculation are those determined independently by Scheraga *et al.*<sup>12</sup> The application of this model calculation has previously been described.<sup>4</sup> Employing these potential functions and the solute and solvent intramolecular force fields, a normal coordinate analysis for a cluster may be numerically determined.<sup>9</sup>

## II. EXPERIMENTAL PROCEDURES

A detailed description of the experimental apparatus and procedures has already been reported.<sup>1</sup> Briefly, the vacuum system consists of two chambers separated by a skimmer and a 2 in. gate valve. The first chamber is used for optical spectroscopy experiments (fluorescence excitation, dispersed emission, and absorption) while the second chamber is used for time-of-flight mass spectroscopy (TOFMS). Both chambers can accommodate pulsed supersonic nozzles. The molecular beam is skimmed before it enters the ionization region of the TOFMS: two separate lasers (two-color) probe and ionize the molecule or cluster.

The proper energy for resonance ( $S_1$ ,  $S_2 \leftarrow S_0$ ) is supplied by two Nd<sup>3+</sup>/YAG pumped dye lasers. The dye laser outputs can be mixed with the Nd<sup>3+</sup>/YAG fundamental (1.064  $\mu\text{m}$ ), doubled, or doubled and mixed to obtain the appropriate ultraviolet energy for the pump-ionization experiment.

The solutes clustered in these experiments are placed inside the pulsed valve head and heated to 35–40 °C in order to increase their vapor pressure. Liquid solvents are placed in a trap behind the pulsed valve; gaseous solvents are pre-mixed with the He expansion gas. Pulsed valve backing pressure is typically 80–100 psi (gauge).

Calculated modeling of the clusters using the LJ potential with its required constants has been previously described.<sup>4,5</sup> Calculations of the normal coordinates and eigenvalues for the cluster vibrational modes are reported in Ref. 9. Both the cluster structure and binding energy calculation and the cluster normal mode calculation have been found to be quite accurate for the test cases of benzene ( $C_n H_{2n+2}$ )<sub>x</sub>, benzene ( $NH_3$ )<sub>x</sub>, benzene ( $H_2O$ )<sub>x</sub>, and for pyridazine clustered with a number of these same solvents. Thus for these new systems (pyridazine and isoquinoline), we have some confidence that the LJ potential and eigenvalue results are at least reliable first approximations for the interpretation of the data presented herein.

## III. RESULTS

Presented in this section are the experimental and calculational results for the pyridazine and isoquinoline clusters. In particular, pyridazine methane and ammonia clusters and

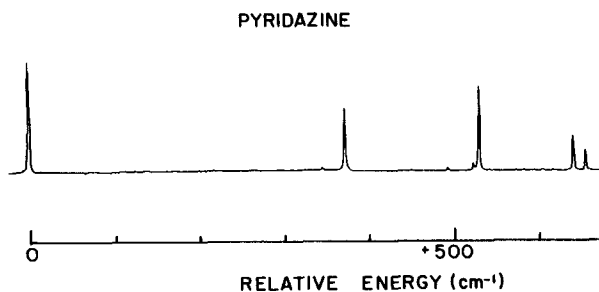


FIG. 1. Time-of-flight mass spectrum (TOFMS) of pyridazine, with the energy scale relative to the  $S_1$  ( $n\pi^*$ )  $0_0^0$  transition at 26 649  $\text{cm}^{-1}$ . The feature at 373  $\text{cm}^{-1}$  to the blue of the  $S_1 0_0^0$  is suggested to be the  $S_2$  ( $n\pi^*$ )  $0_0^0$  transition.

isoquinoline methane, ammonia, methanol, and water clusters are discussed. A normal coordinate analysis of the vdW vibrational modes of pyridazine ammonia is also presented. Calculated geometries and binding energies are presented for many of the configurations available to these clusters. Since the spectra presented are quite complex, at least in principle because of the  $S_1$ – $S_2$  proximity and vibronic coupling, true experimental binding energies are difficult to obtain. In previous experience, the calculated binding energies are always within the limits set by the experimental determinations<sup>1</sup>: the binding energy presented below are those obtained from the calculations.

### A. Pyridazine

Circumstantial evidence cited by Ransom and Innes<sup>6</sup> and by Ito and co-workers<sup>7</sup> support the existence of two  $n\pi^*$  electronic states of pyridazine separated by 373  $\text{cm}^{-1}$ . Figure 1 shows part of the pyridazine monomer spectrum. The first of the two origins is  $S_1$  at 26 649  $\text{cm}^{-1}$  and the second is " $S_2$ " ( $S_1 0_0^0 + 373 \text{ cm}^{-1}$ ) at 27 022  $\text{cm}^{-1}$ . Given these assignments, the feature at 534  $\text{cm}^{-1}$  to the blue of  $S_1$  is suggested to be  $6a_0^1$ . Other possible assignments for the features in this region would be  $10a_0^1$ ,  $10a_0^2$ ,  $6a_0^1$ ,  $6b_0^1$ , etc.

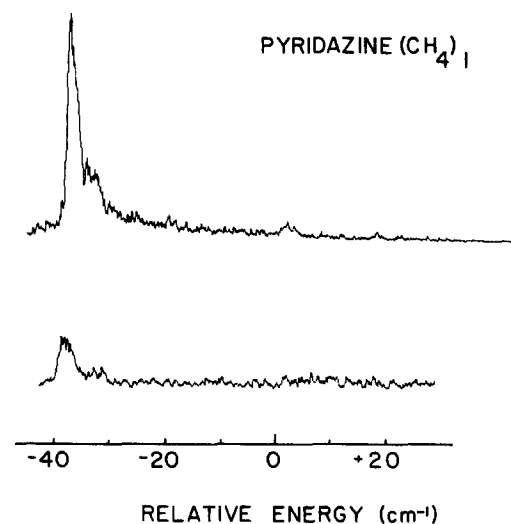


FIG. 2. TOFMS of pyridazine ( $CH_4$ )<sub>1</sub> in the regions of  $S_1$  origin (top spectrum) and suggested  $S_2$  origin (lower spectrum). Both of these pyridazine origins fall at 0  $\text{cm}^{-1}$  on this scale.

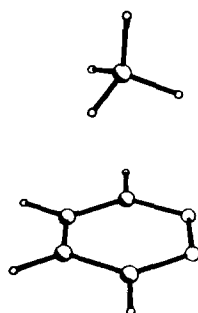
PYRIDAZINE (CH<sub>4</sub>)<sub>1</sub>-513 cm<sup>-1</sup>

FIG. 3. Minimum energy configuration and binding energy for pyridazine (CH<sub>4</sub>)<sub>1</sub> as obtained using a LJ potential calculation.

### B. Pyridazine-methane

The spectra of pyridazine (CH<sub>4</sub>)<sub>1</sub> in the two origin regions are similar to each other and similar to the spectra of pyrazine (CH<sub>4</sub>)<sub>1</sub><sup>4</sup> and pyrimidine (CH<sub>4</sub>)<sub>1</sub>.<sup>5</sup> The upper trace of Fig. 2 is the spectrum of the cluster at the *S*<sub>1</sub> origin and the lower trace is the spectrum of the cluster at the *S*<sub>1</sub> + 373 cm<sup>-1</sup> (*S*<sub>2</sub>) origin. These cluster origins are shifted from the pyridazine free molecule origins by -36.5 and -38.3 cm<sup>-1</sup>, respectively. Low-frequency van der Waals (vdW) vibrational structure occurs at 2.8 and 4.3 cm<sup>-1</sup> from *S*<sub>1</sub> and 5.5 and 7.1 cm<sup>-1</sup> from *S*<sub>2</sub>. Based on our vdW mode normal coordinate analysis for many different clusters,<sup>9</sup> these weak features are almost certainly sequence structure. Weaker features in the spectra are most likely vdW modes of the excited states.

A single configuration is calculated for the stable geometry of the pyridazine (CH<sub>4</sub>)<sub>1</sub> cluster (see Fig. 3). The cluster binding energy is 513 cm<sup>-1</sup>. The methane carbon is 3.5 Å above the center of the ring; one of the methane hydrogen atoms points to the center of the pyridazine N-N bond.

TABLE I. Observed features, shifts, calculated vibrational modes (in cm<sup>-1</sup>), and assignments for the pyridazine (NH<sub>3</sub>)<sub>1</sub> cluster. The two pyridazine "origins" are *S*<sub>1</sub> located at 26 649 cm<sup>-1</sup> and *S*<sub>1</sub> 0<sub>0</sub><sup>0</sup> + 373 cm<sup>-1</sup> (possibly *S*<sub>2</sub>) located at 27 022 cm<sup>-1</sup>.

Energy (vac. cm <sup>-1</sup> )	Energy relative to corresponding pyridazine origin	Energy relative to corresponding pyridazine-ammonia 0 <sub>0</sub> <sup>0</sup>	Energy calculated using normal coordinate analysis	Assignment
27 088.4	439.4	0		II 0 <sub>0</sub> <sup>0</sup> <i>S</i> <sub>1</sub>
27 094.8	445.8	0		I 0 <sub>0</sub> <sup>0</sup> <i>S</i> <sub>1</sub>
27 120.9	471.9	32.5	36.9	II bend
27 127.3	478.3	32.5	29.7	I bend
27 142.0	493.0	53.6	50.0	II tor.
27 144.5	495.5	49.7	58.2	I tor.
27 152.4	503.4	64.0	78.2	II stretch
27 468.5	446.5	0		I 0 <sub>0</sub> <sup>0</sup> <i>S</i> <sub>2</sub>
27 504.9	482.9	36.4		I bend

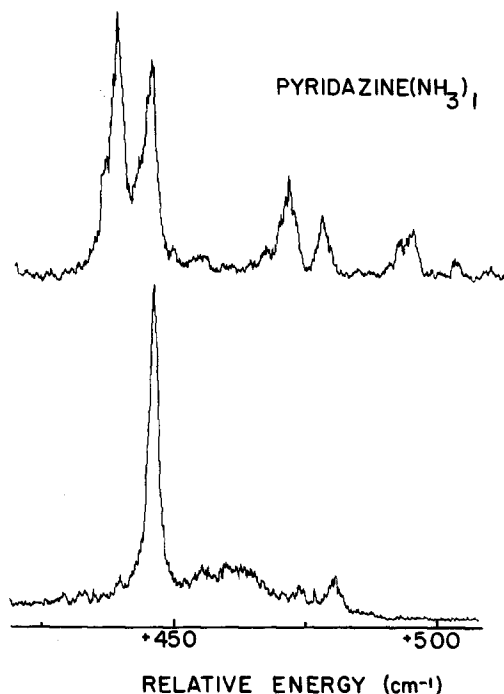


FIG. 4. TOFMS of pyridazine (NH<sub>3</sub>)<sub>1</sub> in the region 450–500 cm<sup>-1</sup> to the blue of *S*<sub>1</sub> (top spectrum) and suggested *S*<sub>2</sub> (lower spectrum) origins.

### C. Pyridazine-ammonia

The two-color TOFMS spectra of pyridazine (NH<sub>3</sub>)<sub>1</sub> show two intense features at 439.4 and 445.8 cm<sup>-1</sup> to the blue of the *S*<sub>1</sub> electronic origin (Fig. 4, top trace). A single intense feature is observed 446.5 cm<sup>-1</sup> to the blue of the *S*<sub>1</sub> + 373 cm<sup>-1</sup> pyridazine feature (Fig. 4, bottom trace). vdW vibrational modes are clearly seen in both traces. The broad feature near the single origin ~460 cm<sup>-1</sup> from the *S*<sub>1</sub> + 373 cm<sup>-1</sup> pyridazine origin might be the missing second cluster (see below) transition: one of the suggested two configurations of pyridazine (NH<sub>3</sub>)<sub>1</sub> could be dissociative at ~ + 450 cm<sup>-1</sup> in the *S*<sub>1</sub> vibronic (or *S*<sub>2</sub>) excited state. Ionization energy has been varied until the cluster features completely disappear with no change in relative peak intensities of any of the pyridazine (NH<sub>3</sub>)<sub>1</sub> features. Table I summarizes these data.

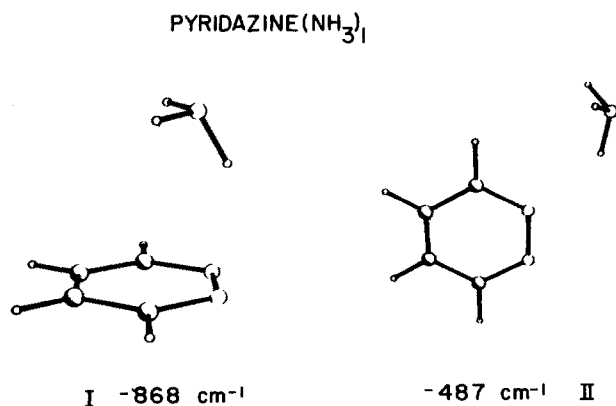


FIG. 5. Minimum energy configurations and binding energies for pyridazine (NH<sub>3</sub>)<sub>1</sub> as obtained using a LJ potential calculation.

Calculations of the geometry, binding energy, and normal modes of vibration of the pyridazine (NH<sub>3</sub>)<sub>1</sub> clusters have been carried out. Figure 5 gives the two stable geometries with their binding energies for this cluster. Configuration I (binding energy 868 cm<sup>-1</sup>) has the ammonia molecule above the pyridazine ring with one hydrogen atom apparently coordinated to the N-N bond. The ammonia nitrogen atom is 3.0 Å above the plane of the aromatic ring and 0.9 Å displaced from the ring center toward the N-N pyridazine bond. The coordinated ammonia hydrogen is situated 2.2 Å above the N-N bond while the other ammonia hydrogens are 3.0 Å above the plane. Configuration II in Fig. 5 has a much smaller binding energy (487 cm<sup>-1</sup>) than does configuration I. In this cluster, one of the ammonia N-H bonds is in the plane of the pyridazine ring with the ammonia nitrogen atom displaced in the plane by ~3.1 Å along both the *x* and *y* axes. Identification of these two calculated geometries with the spectroscopic observations above will be presented in the Discussion section along with the assignment of the vdW modes to torsions, bends, or stretches.

#### D. Isoquinoline

The region 3135 to 3080 Å of the isoquinoline spectrum is displayed in Fig. 6. The  $n\pi^*$  origin of isoquinoline ( $S_1$ ) occurs at 30 821 cm<sup>-1</sup> (3244.5 Å—not shown in Fig. 6) and is of very low intensity. The  $S_2$  ( $\pi\pi^*$ ) origin is assigned as

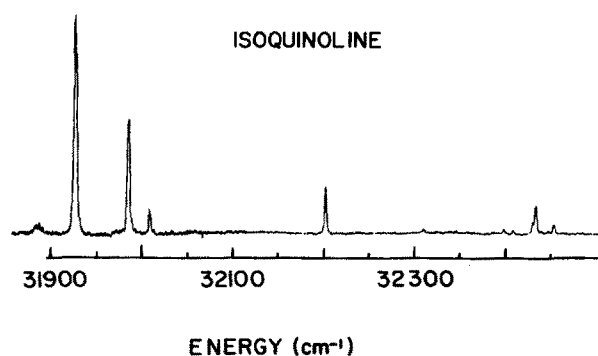


FIG. 6. TOFMS of isoquinoline in the region of the  $S_2$  ( $\pi\pi^*$ ) transition the origin of which occurs at 31 929 cm<sup>-1</sup>.

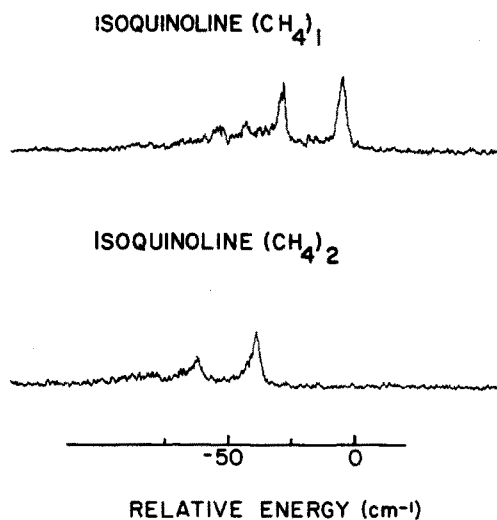


FIG. 7. TOFMS of isoquinoline (CH<sub>4</sub>)<sub>1</sub> and isoquinoline (CH<sub>4</sub>)<sub>2</sub> in the region of the isoquinoline  $S_2$  ( $\pi\pi^*$ )  $0_0^0$  transition (31 929 cm<sup>-1</sup>). The scale is relative to the isoquinoline  $S_2$  ( $\pi\pi^*$ )  $0_0^0$  transition.

the intense peak at 31 929 cm<sup>-1</sup> in Fig. 6. The features at 31 987 and 32 010 cm<sup>-1</sup> in the figure are reported to arise from vibronic coupling of two  $a''$  vibronic levels of the  $S_1$  ( $n\pi^*$ ) state with the  $S_2$  ( $\pi\pi^*$ ) origin.<sup>11</sup>

#### E. Isoquinoline-methane

The isoquinoline (CH<sub>4</sub>)<sub>1</sub> cluster spectrum shows two main features at 27.8 and 4.6 cm<sup>-1</sup> to the red of the isoquinoline  $\pi\pi^*$  origin (Fig. 7). The isoquinoline (CH<sub>4</sub>)<sub>2</sub> cluster spectrum also has two main features to the red of the isoquinoline  $S_2$  ( $\pi\pi^*$ ) origin at -61.2 and -37.7 cm<sup>-1</sup>. Weaker features can be seen in both spectra both to the red and blue of the  $S_2$  ( $\pi\pi^*$ ) isoquinoline feature. These data are tabulated in Table II.

Intermolecular potential energy calculations for isoquinoline-methane cluster geometries are depicted in Fig. 8 along with their binding energies. The isoquinoline (CH<sub>4</sub>)<sub>1</sub> cluster is calculated to have only one configuration (binding energy 702 cm<sup>-1</sup>) with the carbon atom of methane centered above the C-C bond common to both rings, and 3.4 Å above the ring plane. The three methane hydrogen atoms that point toward the ring are at 3.0 Å above it. Two minimum energy stable equilibrium configurations are calculated for isoquinoline (CH<sub>4</sub>)<sub>2</sub>. As has been the case for other aromatic systems,<sup>1-5</sup> these configurations have methane on

TABLE II. Observed peaks in the spectra of isoquinoline-methane.

Species	Energy (vac. cm <sup>-1</sup> )	Energy relative to $\pi\pi^*$ origin of isoquinoline (cm <sup>-1</sup> )
C <sub>9</sub> H <sub>7</sub> N(CH <sub>4</sub> ) <sub>1</sub>	31 876.5	- 52.5
	31 886.7	- 42.3
	31 901.2	- 27.8
	31 924.4	- 4.6
C <sub>9</sub> H <sub>7</sub> N(CH <sub>4</sub> ) <sub>2</sub>	31 867.8	- 61.2
	31 891.3	- 37.7

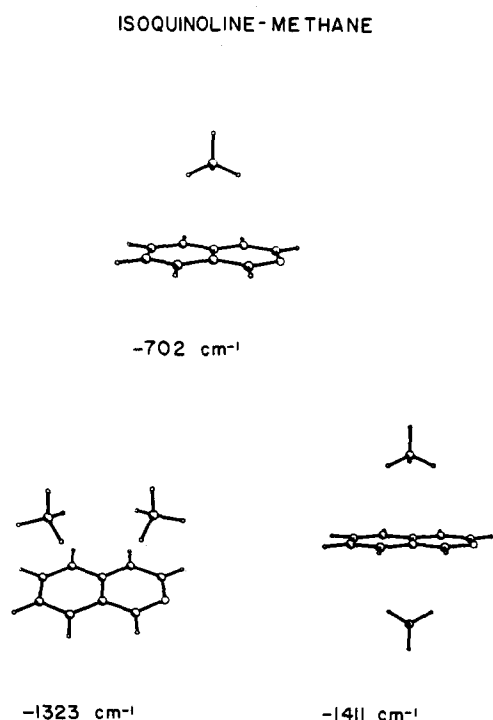


FIG. 8. Minimum energy configurations and binding energies for isoquinoline  $(\text{CH}_4)_1$  and isoquinoline  $(\text{CH}_4)_2$  as obtained using a LJ potential calculation.

the same and opposite sides of the ring. The asymmetrical configuration has carbon atoms of the methane molecule 3.5 Å above the plane and 1.8 Å displaced from the ring system center above each ring. The binding energy for this configuration is 1323  $\text{cm}^{-1}$ . The symmetrical configuration of isoquinoline  $(\text{CH}_4)_2$  has a 1411  $\text{cm}^{-1}$  binding energy and configuration for the methane molecules exactly as found for isoquinoline  $(\text{CH}_4)_1$ .

### F. Isoquinoline-ammonia

Isoquinoline-ammonia cluster spectra are displayed in Figs. 9 and 10 for one and two ammonias, respectively. Table III gives the energies and relative shifts for all the features with respect to the  $S_2$  ( $\pi\pi^*$ ) origin. The isoquinoline  $(\text{NH}_3)_1$  spectrum has two intense features at 31 934.5 and 31 952.4  $\text{cm}^{-1}$  with shifts of 5.5 and 23.4  $\text{cm}^{-1}$  to the blue of

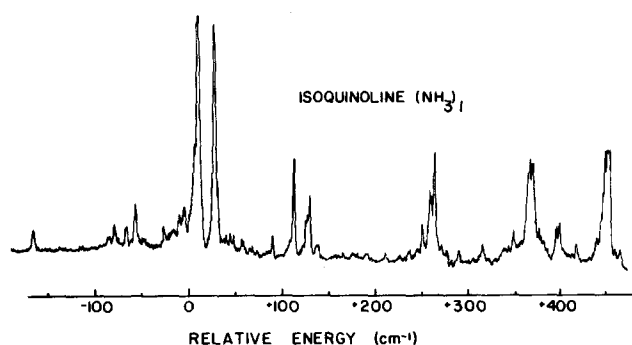


FIG. 9. TOFMS of isoquinoline  $(\text{NH}_3)_1$  in the region of the isoquinoline  $S_2$  ( $\pi\pi^*$ )  $0_0^0$  transition (31 929  $\text{cm}^{-1}$ ), which corresponds to 0  $\text{cm}^{-1}$  on this scale.

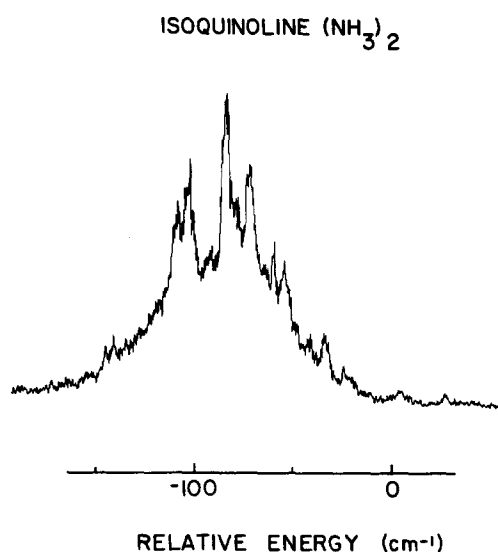


FIG. 10. TOFMS of isoquinoline  $(\text{NH}_3)_2$  in the region of the isoquinoline  $S_2$  ( $\pi\pi^*$ ) transition (31 929  $\text{cm}^{-1}$ ), which corresponds to 0  $\text{cm}^{-1}$  on this scale.

the isoquinoline  $S_2$  origin. Extensive van der Waals vibrational structure appears following these features; however, comparison with the other ammonia aromatic and heteroaromatic cluster systems<sup>5</sup> suggests that this is probably not more than 450  $\text{cm}^{-1}$  of irregular vdW mode intensity. Note that the apparent vdW mode intensity is largest at 450  $\text{cm}^{-1}$  from the cluster origins.

The cluster spectra for isoquinoline  $(\text{NH}_3)_2$  clusters are completely different from those of the isoquinoline  $(\text{NH}_3)_1$  clusters. These spectra, displayed in Fig. 10, consist of a broad background at a shift of  $\sim -100$   $\text{cm}^{-1}$  from the  $\pi\pi^*$  origin with superimposed sharp features and little vdW mode intensity in a short progression.

TABLE III. Observed peaks in the spectra of isoquinoline-ammonia.

Species	Energy (vac. $\text{cm}^{-1}$ )	Energy relative to $\pi\pi^*$ origin of isoquinoline ( $\text{cm}^{-1}$ )
$\text{C}_9\text{H}_7\text{N}(\text{NH}_3)_1$	31 757.7	- 171.3
	31 843.4	- 85.6
	31 856.4	- 72.6
	31 865.7	- 63.3
	31 895.9	- 33.1
	31 918.5	- 10.5
	31 934.5	5.5
	31 952.4	23.4
	32 015.0	86.0
	32 037.9	108.9
	32 055.5	126.5
	32 063.8	134.8
	32 179.5	250.5
	32 187.7	258.7
	32 193.1	264.1
32 298.8	369.8	
32 332.8	403.8	
32 385.0	456.0	
$\text{C}_9\text{H}_7\text{N}(\text{NH}_3)_2$	31 823.5	- 105.5
	31 843.3	- 85.7
	31 855.2	- 73.8

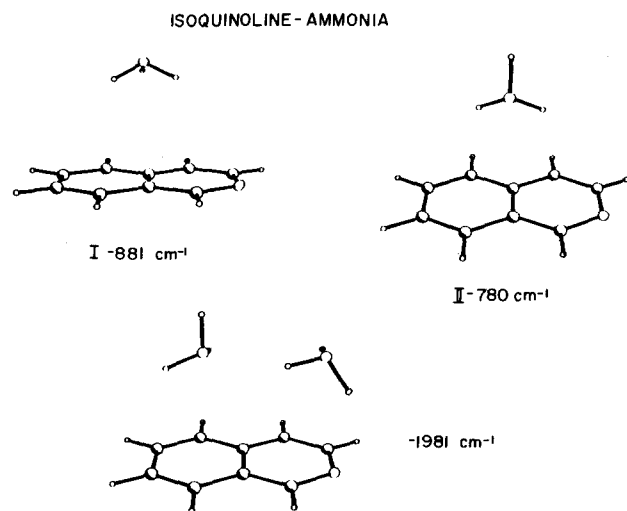


FIG. 11. Minimum energy configurations and binding energies for isoquinoline  $(\text{NH}_3)_1$  and isoquinoline  $(\text{NH}_3)_2$  as obtained using a LJ potential calculation.

Potential calculations for isoquinoline  $(\text{NH}_3)_1$  yield two configurations with binding energies of 881 and 780  $\text{cm}^{-1}$  (see Fig. 11). Configuration I has the three ammonia hydrogen atoms pointing down toward the ring with one of them oriented in the direction of the ring nitrogen atom. The nitrogen atom of ammonia in this cluster is 3.2 Å above the C-C bond common to the two rings. Configuration II has two hydrogens of the ammonia molecule pointed toward the ring and again the ammonia nitrogen is centered on the ring common C-C bond 3.2 Å above the ring plane. This cluster has a roughly 100  $\text{cm}^{-1}$  smaller binding energy than cluster I.

A number of possible configurations arise for the isoquinoline  $(\text{NH}_3)_2$  system. All symmetrical and "mixed" symmetrical clusters are of course possible. The cluster calculated and displayed in Fig. 11 has an asymmetrical structure and is roughly a mixture of the two isoquinoline  $(\text{NH}_3)_1$  configurations. The structure has a binding energy of nearly 2000  $\text{cm}^{-1}$ . Other asymmetrical configurations for the isoquinoline  $(\text{NH}_3)_2$  clusters most likely exist: we have not explored the entire surface of this system.

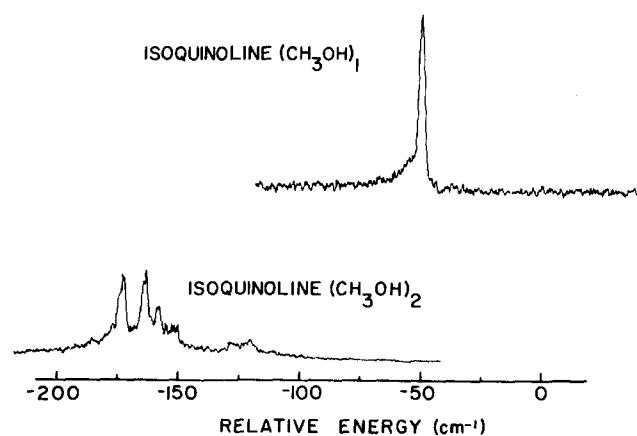


FIG. 12. TOFMS of isoquinoline  $(\text{CH}_3\text{OH})_1$  and isoquinoline  $(\text{CH}_3\text{OH})_2$  in the region of the isoquinoline  $S_2$  ( $\pi\pi^*$ )  $0_0^0$  transition (31 929  $\text{cm}^{-1}$ ), which corresponds to 0  $\text{cm}^{-1}$  on this scale.

TABLE IV. Observed peaks in the spectra of isoquinoline-methanol.

Species	Energy (vac. $\text{cm}^{-1}$ )	Energy relative to $\pi\pi^*$ origin of isoquinoline ( $\text{cm}^{-1}$ )
$\text{C}_9\text{H}_7\text{N}(\text{CH}_3\text{OH})_1$	31 879.8	- 49.2
$\text{C}_9\text{H}_7\text{N}(\text{CH}_3\text{OH})_2$	31 756.5	- 172.5
	31 766.0	- 163.0
	31 771.8	- 157.2
	31 777.8	- 151.2
	31 804.4	- 124.6
	31 811.2	- 117.8

### G. Isoquinoline-methanol

The isoquinoline  $(\text{CH}_3\text{OH})_1$  cluster spectrum is very simple (see Fig. 12). It consists of a single sharp feature at 49.2  $\text{cm}^{-1}$  to the red of the  $S_2$  ( $\pi\pi^*$ ) isoquinoline origin at 31 929  $\text{cm}^{-1}$ . No vdW mode features are observed for this cluster. Previously reported spectra for this cluster<sup>13,14</sup> using fluorescence excitation and concentration variation to detect and identify the isoquinoline  $(\text{CH}_3\text{OH})_1$  are not correct. The isoquinoline  $(\text{CH}_3\text{OH})_2$  clusters have features with red shifts between  $\sim 175$  to 125  $\text{cm}^{-1}$  from  $S_2$  ( $\pi\pi^*$ ) origin. Table IV gives these energies and relative shifts.

A single configuration is calculated for the isoquinoline  $(\text{CH}_3\text{OH})_1$  cluster: it is depicted in Fig. 13. The OH group of methanol is over the heteroaromatic ring with the hydrogen of the OH group coordinated to the nitrogen of the isoquinoline ring. The suggested geometry indicates that the  $\pi$ -system and  $\text{CH}_3$  interact and the nitrogen lone pair and OH hydrogen form a hydrogen bond. Many configurations are expected for isoquinoline  $(\text{CH}_3\text{OH})_2$  and detailed calculations have not as yet been carried out for this system, as the experimental spectra do not afford a ready assignment.

### H. Isoquinoline-water

Clusters of isoquinoline with one, two, and three water molecules are observed and identified by two-color TOFMS. Figure 14 shows the spectrum of isoquinoline  $(\text{H}_2\text{O})_1$  (top) and isoquinoline  $(\text{H}_2\text{O})_2$  (bottom) clusters, and Fig. 15 presents the spectrum of isoquinoline  $(\text{H}_2\text{O})_3$ . Table V lists the various major intensity water cluster features and their shifts

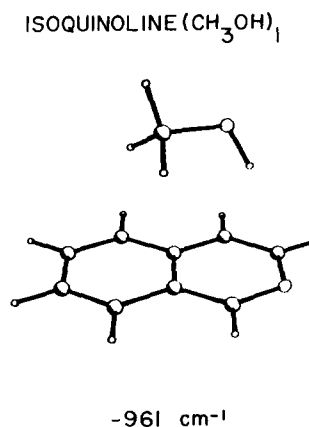


FIG. 13. Minimum energy configuration and binding energy for isoquinoline  $(\text{CH}_3\text{OH})_1$  as obtained using a LJ potential calculation.

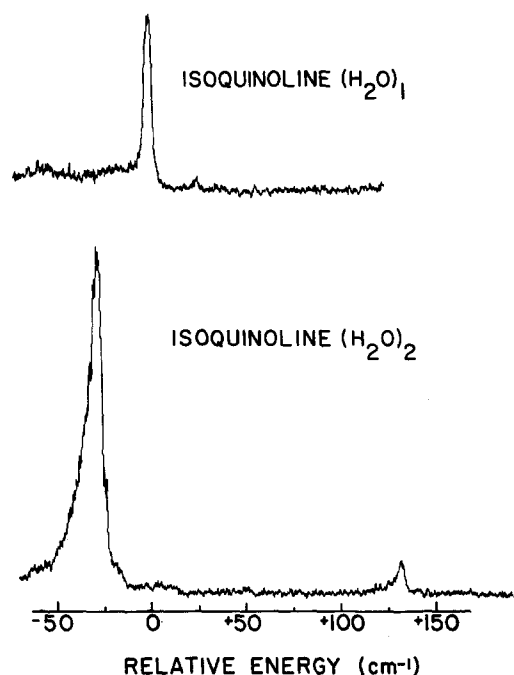


FIG. 14. TOFMS of isoquinoline ( $\text{H}_2\text{O}$ )<sub>1</sub> and isoquinoline ( $\text{H}_2\text{O}$ )<sub>2</sub> in the region of the isoquinoline  $S_2$  ( $\pi\pi^*$ )  $0_0^0$  transition ( $31\,929\text{ cm}^{-1}$ ), which corresponds to  $0\text{ cm}^{-1}$  on this scale.

with respect to the  $S_2$  ( $\pi\pi^*$ ) isoquinoline origin at  $31\,929\text{ cm}^{-1}$ .

Isoquinoline ( $\text{H}_2\text{O}$ )<sub>1</sub> has a single intense feature at  $31\,929.6\text{ cm}^{-1}$  almost overlapping with the  $\pi\pi^*$  monomer origin. If mass detection were not employed, this species would not be observed. A weak feature can be seen  $25.9\text{ cm}^{-1}$  to the blue of the cluster origin. The cluster spectrum of isoquinoline ( $\text{H}_2\text{O}$ )<sub>2</sub> consists of two features, an intense one at  $31\,899.4$  or  $29.6\text{ cm}^{-1}$  to the red of the isoquinoline  $S_2$  ( $\pi\pi^*$ ) origin and a weak one at  $128.7\text{ cm}^{-1}$  to the blue of the  $S_2$  ( $\pi\pi^*$ ) monomer origin.

The isoquinoline ( $\text{H}_2\text{O}$ )<sub>3</sub> cluster spectrum (Fig. 15) is indeed very different from the two previous ones. Many features are observed between  $-125$  and  $+350\text{ cm}^{-1}$  about the isoquinoline  $S_2$  origin. The spectra suggest both vdW mode intensity and several different cluster configurations. The previously reported isoquinoline water spectra (fluorescence excitation detected)<sup>14</sup> do not coincide with the two-color TOFMS spectra reported here.

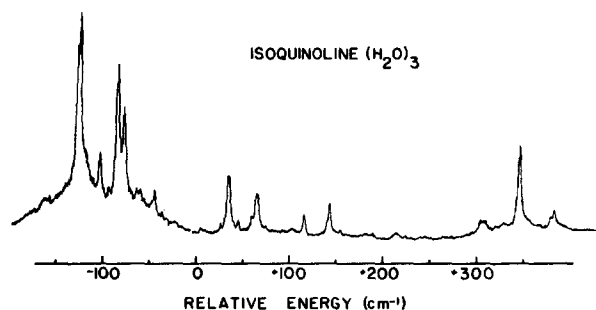


FIG. 15. TOFMS of isoquinoline ( $\text{H}_2\text{O}$ )<sub>3</sub> in the region of the isoquinoline  $S_2$  ( $\pi\pi^*$ )  $0_0^0$  transition ( $31\,929\text{ cm}^{-1}$ ), which corresponds to  $0\text{ cm}^{-1}$  on this scale.

TABLE V. Observed peaks in the spectra of isoquinoline-water.

Species	Energy (vac. $\text{cm}^{-1}$ )	Energy relative to $\pi\pi^*$ origin of isoquinoline ( $\text{cm}^{-1}$ )
$\text{C}_9\text{H}_7\text{N}(\text{H}_2\text{O})_1$	31 929.6	0.6
	31 954.9	25.9
$\text{C}_9\text{H}_7\text{N}(\text{H}_2\text{O})_2$	31 899.4	- 29.6
	32 057.7	128.7
$\text{C}_9\text{H}_7\text{N}(\text{H}_2\text{O})_3$	31 804.1	- 124.9
	31 826.4	- 102.6
	31 845.1	- 83.9
	31 852.1	- 76.9
	31 963.0	34.0
	31 993.4	64.4
	32 045.5	116.5
	32 073.5	144.5
	32 281.6	352.6

Calculated configurations for these clusters are presented in Figs. 16 and 17 with their binding energies. Two geometries are generated for the isoquinoline ( $\text{H}_2\text{O}$ )<sub>1</sub> cluster with very similar binding energies. Configurations I and II have similar oxygen positions for the water molecule ( $3.0\text{ \AA}$  above the different rings) but different orientations of the water hydrogen atoms. The water over the heterocyclic ring (configuration II) has one hydrogen tipped toward the ring nitrogen atom.

Four calculated configurations are obtained for the isoquinoline ( $\text{H}_2\text{O}$ )<sub>2</sub> clusters. Three of these are presented in Fig. 17. The two symmetrical ones are simply additive configurations based on the isoquinoline ( $\text{H}_2\text{O}$ )<sub>1</sub> geometries. A third configuration arises from the mixed symmetric cluster. The asymmetric configuration with both waters on the same side of the ring has a very large binding energy mostly because of the formation of a water dimer in this structure.

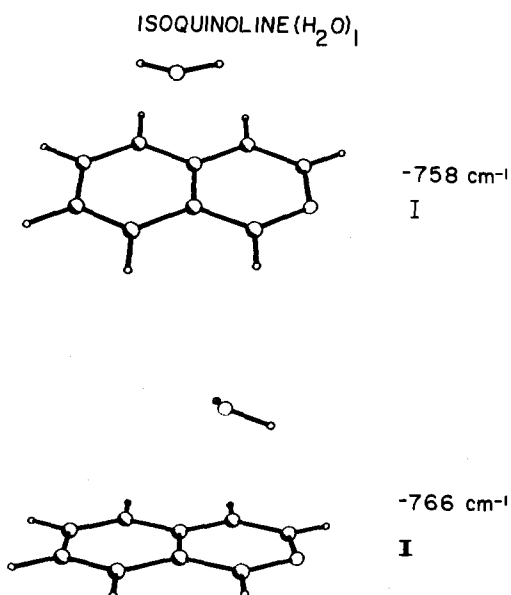


FIG. 16. Minimum energy configurations and binding energies for isoquinoline ( $\text{H}_2\text{O}$ )<sub>1</sub> as obtained using a LJ potential calculation.

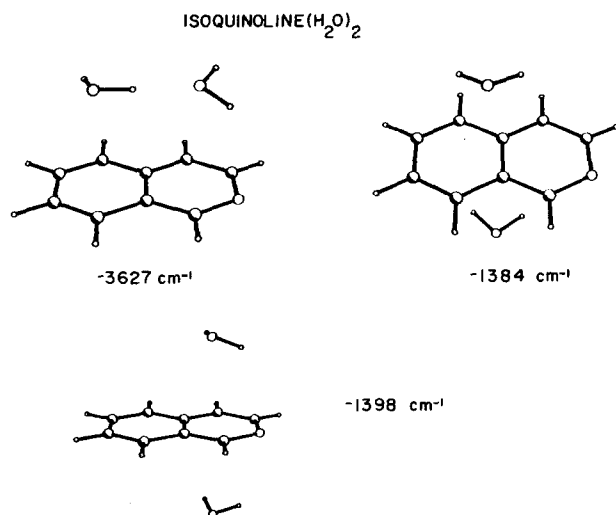


FIG. 17. Minimum energy configurations and binding energies for isoquinoline ( $\text{H}_2\text{O}$ )<sub>2</sub> as obtained using a LJ potential calculation.

No attempts have been made as yet to calculate geometries and binding energies for the numerous isoquinoline ( $\text{H}_2\text{O}$ )<sub>3</sub> clusters.

#### IV. DISCUSSION

In this section we will confine our remarks to four main areas: (1) comparisons with similar clusters previously studied (e.g., pyrazine and pyrimidine clusters); (2) correlation between the observed spectra and the calculated geometries for a given cluster; (3) the nature of the pyridazine  $S_1 + 373 \text{ cm}^{-1}$  feature as evidenced by clustering; and (4) the effect of solvation on the  $n\pi^* - \pi\pi^*$  excited state vibronic coupling in isoquinoline clusters.

Recall that the diazines do not in general have observable  $n\pi^*$  transitions in strongly hydrogen bonded clusters.<sup>5</sup> Thus we have not been able to observe clusters of pyridazine with either water or methanol in these experiments.

##### A. Pyridazine-methane

Pyridazine ( $\text{CH}_4$ )<sub>1</sub> spectra are very similar to those of pyrazine and pyrimidine ( $\text{CH}_4$ )<sub>1</sub> both at the  $S_1$  ( $n\pi^*$ ) and  $S_1 + 373 \text{ cm}^{-1}$  ( $n\pi^*$ ) origins. Little vdW vibronic intensity is observed except for what must be sequence bands following the origins. In all cases the cluster shifts are quite similar (see Fig. 2).

Only one configuration is calculated for this cluster: the predicted geometry is the same in all three diazine-methane clusters.<sup>4,5</sup> All evidence strongly suggests that the methane coordinates to the ring aromatic  $\pi$ -system, as depicted in Fig. 3. The calculated and experimentally bracketed binding energies are in complete agreement ( $\sim 500 \text{ cm}^{-1}$ ).

The pyridazine ( $\text{CH}_4$ )<sub>1</sub> cluster does not definitively suggest the nature of the  $S_2$  ( $= S_1 + 373 \text{ cm}^{-1}$ ) origin.

##### B. Pyridazine-ammonia

Ammonia clusters with the three diazines<sup>5</sup> have now been studied: all three clusters have large blue ( $+100$  to  $+500 \text{ cm}^{-1}$ ) shifts with respect to the solute origins. As

expected for an  $n\pi^*$  transition in a weakly hydrogen bonding system, the excited state of the cluster is destabilized with respect to the ground state. Both pyridazine and pyrimidine ( $\text{NH}_3$ )<sub>1</sub> clusters show evidence for multiple configurations (see Fig. 4). The intensity at the cluster  $S_1$  origin suggests that the pyridazine ( $\text{NH}_3$ )<sub>1</sub> cluster has two different configurations. In fact, two configurations for this cluster are calculated and presented in Fig. 5. These clusters are described in the Results section and have quite different binding energies and geometries. On the other hand, the  $S_1 + 373 \text{ cm}^{-1}$  origin evidences only one clear configuration: the missing feature may be the broad structure to the blue of the sharp feature at  $S_2 + 446.5 \text{ cm}^{-1}$ . Since the calculations suggest that the two structures have binding energies of 870 and 490  $\text{cm}^{-1}$ , we conclude that the lower binding energy configuration II (Fig. 5) cluster is dissociative at this energy. This configuration has the smallest binding energy for any diazine ( $\text{NH}_3$ )<sub>1</sub> structure.

Assuming that the  $S_1 + 373 \text{ cm}^{-1}$  is an  $S_2$  ( $n\pi^*$ ) origin the configuration II cluster would have to be dissociative on the excited electronic state potential surface. If  $S_2$  is really a vibronic feature of  $S_1$  (e.g.,  $10a_0^1$ ,  $6a_0^1$ , etc.), then vibrational predissociation could account for the loss of spectrum at this energy once the  $373 \text{ cm}^{-1}$  of vibrational energy is transferred to the vdW cluster modes. The binding energy in  $S_1$  is  $\sim 450 \text{ cm}^{-1}$  smaller than that in  $S_0$ : this would account for the dissociation with  $373 \text{ cm}^{-1}$  in the vdW modes based on the  $\sim 490 \text{ cm}^{-1}$  calculated  $S_0$  binding energy for cluster II.

These cluster spectra do not prove either possible assignment for the  $S_1 + 373 \text{ cm}^{-1}$  feature, although the more likely candidate is a vibronic  $S_1$  feature based on cluster shift similarity with the  $S_1 0_0^0$ . We also believe that the cluster  $S_2$  excited state would probably not be dissociative at the  $S_2 0_0^0$ . In either event, the remaining cluster at  $S_1 + 373 \text{ cm}^{-1}$  most likely is configuration I with the large ( $\sim 890 \text{ cm}^{-1}$ ) binding energy. The cluster spectra are then assigned to the calculated configuration: configuration I has both the larger binding energy and the larger blue shift.

Since the pyridazine ( $\text{NH}_3$ )<sub>1</sub> clusters are one of the few in this series to evidence clear vibronic vdW structure, a normal coordinate analysis of these clusters is presented. The methods and techniques are discussed in previously published reports.<sup>9</sup> The results of the calculations lead to the vdW mode assignments given in Table I. As has been found for other vdW mode vibronic spectra,<sup>9</sup> most of the vibrational mode intensity is in the bending and torsional modes of the cluster. A low intensity vdW mode stretch has been assigned to configuration II (see Table I and Fig. 4).

##### C. Isoquinoline-methane

As has been demonstrated for diazines, coordination of an aromatic system with a  $n\pi^*$  excited state by an alkane molecule does not shift the spectrum more than  $\sim 100 \text{ cm}^{-1}$  to the red. Thus, one can expect that an isoquinoline ( $\text{CH}_4$ )<sub>1</sub> cluster should evidence both its  $n\pi^*$  and  $\pi\pi^*$  electronic transitions in more or less the same spectral region as does the isoquinoline monomer. The calculated configuration for isoquinoline ( $\text{CH}_4$ )<sub>1</sub> is presented in Fig. 8: only one minimum energy configuration is found. In other systems,<sup>1-5</sup> aromatic

molecule–methane cluster calculations are always in agreement with conclusions from experimentally observed cluster spectra, especially with respect to the number of different cluster configurations. We are thus led to suggest that the isoquinoline  $(\text{CH}_4)_1$  spectrum is, like isoquinoline spectrum itself, a composite of  $S_1$  ( $n\pi^*$ ) and  $S_2$  ( $\pi\pi^*$ ) intensity. The cluster does not greatly perturb the vibronic interaction between these manifolds and the spectrum is thus a reflection of this interaction and not the number of cluster geometrical configurations with vdW mode structure built on them. Moreover, no additive shift relation exists for the isoquinoline  $(\text{CH}_4)_1$  and  $(\text{CH}_4)_2$  clusters and thus we conclude that the isoquinoline  $(\text{CH}_4)_2$  spectra are also a composition of  $S_1$  and  $S_2$  transitions. Thus these data only reflect the small perturbation that clustering in this instance has on the  $S_1$  ( $n\pi^*$ )– $S_2$  ( $\pi\pi^*$ ) vibronic interaction.

#### D. Isoquinoline–ammonia

Two configurations are calculated for the isoquinoline  $(\text{NH}_3)_1$  cluster and apparently two intense features near the isoquinoline  $S_2$  ( $\pi\pi^*$ ) state origin are observed. While these features probably are associated with the two cluster origins, the nearly  $500\text{ cm}^{-1}$  of apparent cluster vibronic spectrum (both to the red and blue of the origins) clearly suggests that  $S_1$  ( $n\pi^*$ )– $S_2$  ( $\pi\pi^*$ ) vibronic coupling and intensity borrowing are important in these observations. Surely some of this structure is vdW mode intensity but firm assignments are not at present possible. We can only conclude that coordination by ammonia is not sufficient to decouple the two electronic states: ammonia is not a very strong hydrogen bonding solvent and does not significantly shift the  $n\pi^*$  state with respect to the  $\pi\pi^*$  state.

Isoquinoline  $(\text{NH}_3)_2$  spectra are of a different nature, as displayed in Fig. 10. Whether this spectrum represents the true  $S_2$  ( $\pi\pi^*$ ) origin of the cluster(s) or a strong vibronic interaction between  $S_1$  and  $S_2$  still exists between these two states is not at all clear. Although only the asymmetric isoquinoline  $(\text{NH}_3)_2$  cluster is presented in Fig. 11, many others, especially symmetric structures, certainly exist.

#### E. Isoquinoline–methanol

The spectrum of isoquinoline  $(\text{CH}_3\text{OH})_1$  (Fig. 12) has only one origin and no vibronic structure: apparently the  $S_1$  ( $n\pi^*$ ) state has been greatly shifted (to the blue, presumably) by the O–H $\cdots$ N hydrogen bonding (Fig. 13) leaving only the uncoupled  $S_2$  ( $\pi\pi^*$ ) state for spectroscopic observation in this region. This origin is red shifted by  $49\text{ cm}^{-1}$  with respect to the  $S_2$  ( $\pi\pi^*$ ) state of the free isoquinoline molecule. The  $\pi$  system, as evidence by  $S_2$  behavior, is little affected by the hydrogen bonding: the cluster  $S_2$  ( $\pi\pi^*$ ) shift is thus mostly controlled by the aromatic hydrocarbon interaction associated with the methyl moiety.

The isoquinoline  $(\text{CH}_3\text{OH})_2$  spectrum is more complicated than the isoquinoline  $(\text{CH}_3\text{OH})_1$  spectrum. The large red shift and the number of features suggest asymmetric configurations are the dominant cluster form. Most likely a number of possible geometries have stable energy minima.

The above observations support the  $S_1$  ( $n\pi^*$ ) and  $S_2$

( $\pi\pi^*$ ) state assignments and their vibronic interaction in this region.

#### F. Isoquinoline–water

The spectroscopic behavior of isoquinoline water clusters is in general similar to that just described for isoquinoline methanol clusters. The isoquinoline  $S_1$  ( $n\pi^*$ ) electronic state has been shifted (perhaps thousands of  $\text{cm}^{-1}$ ) to the blue, out of resonance with the  $S_2$  ( $\pi\pi^*$ ) state whose origin is observed for the various clusters. For isoquinoline  $(\text{H}_2\text{O})_1$  and  $(\text{H}_2\text{O})_2$  clusters, little vibronic intensity is observed. The  $(\text{H}_2\text{O})_1$  cluster has almost no shift for the  $S_2$  ( $\pi\pi^*$ ) state, whereas the  $(\text{H}_2\text{O})_2$  and  $(\text{H}_2\text{O})_3$  clusters have significant red shifts (see Table V). With the exception of the cluster shift, the  $(\text{H}_2\text{O})_1$  and  $(\text{H}_2\text{O})_2$  clusters have very similar spectra. The feature in the  $(\text{H}_2\text{O})_2$  spectrum at  $\sim +128\text{ cm}^{-1}$  from the isoquinoline origin is most likely another cluster geometry rather than a vdW mode vibronic feature because such an intensity distribution in cluster vdW mode spectra would be quite unusual. The calculations for both these clusters suggest multiple configurations are present in the spectroscopic observations. The two configurations for isoquinoline  $(\text{H}_2\text{O})_1$  are separated by a barrier of less than  $30\text{ cm}^{-1}$ : their cluster shifts might be nearly identical, giving rise to the spectrum presented in the top trace of Fig. 14. The water dimer asymmetric configuration for isoquinoline  $(\text{H}_2\text{O})_2$  (Fig. 16) will probably be the most abundant in the expansion at this mass and may therefore be responsible for the  $-30\text{ cm}^{-1}$  intense feature in the bottom trace of the Fig. 14. The other three possible  $(\text{H}_2\text{O})_2$  clusters (only two of which are displayed in Fig. 16) may well contribute to the  $+129\text{ cm}^{-1}$  intensity in the isoquinoline  $(\text{H}_2\text{O})_2$  spectrum.

The isoquinoline  $(\text{H}_2\text{O})_3$  spectrum is quite complex suggesting many different configurations and possibly vdW vibronic mode structure. The  $S_1$  ( $n\pi^*$ )– $S_2$  ( $\pi\pi^*$ ) interaction is not expected to be important here as is the case for the other isoquinoline water clusters; therefore, all observed structure is associated with the  $S_2$  ( $\pi\pi^*$ )  $(\text{H}_2\text{O})_3$  cluster spectra. Calculations have not been attempted for this system.

#### V. CONCLUSIONS

Mass detected optical spectroscopy of pyridazine and isoquinoline clustered with  $\text{CH}_4$ ,  $\text{NH}_3$ ,  $\text{CH}_3\text{OH}$ , and  $\text{H}_2\text{O}$  has led to a number of insights with regard to solute/solvent interactions and the affect of solvation on solute electronic states and their interactions. Both solutes in this instance are reported to have two electronic states, both  $n\pi^*$  for pyridazine and  $n\pi^*$  and  $\pi\pi^*$  for isoquinoline, close to one another which vibronically couple. Our results support without question this contention for isoquinoline; but for pyridazine our results would agree more with the notion that only one  $n\pi^*$  excited singlet state is spectroscopically observed near  $26\,000\text{ cm}^{-1}$ .

Clusters of diazines with hydrocarbons seem to be similar with regard to spectroscopy and calculated configurations. The experimental data seem consistent with expectations based on computer modeling. Ammonia on the other

hand generates cluster spectra and geometry that differ for all three diazines. The nitrogen positions in the heterocyclic ring seem to affect the weak  $\text{NH}_3 \cdots \text{N}$  hydrogen bonding interaction significantly.

A complete intermolecular normal coordinate analysis of the pyridazine  $(\text{NH}_3)_1$  cluster has led to assignment of all spectroscopic vdW mode vibronic features for this cluster.

Weakly hydrogen bonding solvents such as ammonia interact with the aromatic ring of isoquinoline much like hydrocarbons do. The geometry predicted and the observed spectra for isoquinoline  $(\text{NH}_3)_{1,2}$  clusters are in substantial agreement with such systems as benzene–ammonia.<sup>5</sup> Methane and ammonia solvation of isoquinoline do change the  $S_1$  ( $n\pi^*$ )– $S_2$  ( $\pi\pi^*$ ) vibronic coupling but only qualitatively: in fact, the coupling appears to be enhanced for the  $(\text{NH}_3)_1$  cluster. Strong hydrogen bonding solvents like methanol and water completely remove the vibronic interaction between these two electronic states: the  $S_1$  ( $n\pi^*$ ) state is probably blue shifted thousands of  $\text{cm}^{-1}$  by the  $\text{O}-\text{H} \cdots \text{N}$  interaction. These cluster spectra are only observed for an isolated  $S_2$  ( $\pi\pi^*$ ) origin.

In all cases, the calculations predict that the interaction between isoquinoline and the solvent is a mixture of  $\pi$ -system interaction with the major solvent electron density and nitrogen lone pair–hydrogen bonding interaction. This is

quite clear in isoquinoline–methanol and –water clusters. Note that both the oxygen atom of water and the methyl groups of methanol coordinate well to the isoquinoline  $\pi$  system. The spectra qualitatively agree with this conclusion based on shifts, binding energies, and intersystem comparisons.

<sup>1</sup>M. Schauer and E. R. Bernstein, *J. Chem. Phys.* **82**, 726 (1985).

<sup>2</sup>M. Schauer, K. S. Law, and E. R. Bernstein, *J. Chem. Phys.* **82**, 736 (1985).

<sup>3</sup>K. S. Law and E. R. Bernstein, *J. Chem. Phys.* **82**, 2856 (1985).

<sup>4</sup>J. Wanna and E. R. Bernstein, *J. Chem. Phys.* **84**, 927 (1986).

<sup>5</sup>J. Wanna, J. A. Menapace, and E. R. Bernstein, *J. Chem. Phys.* **85**, 1795 (1986).

<sup>6</sup>B. D. Ransom and K. K. Innes, *J. Mol. Spectros.* **69**, 394 (1978).

<sup>7</sup>E. Ueda, Y. Udagawa, and M. Ito, *Chem. Lett.* **1981**, 873.

<sup>8</sup>M. Terazima, S. Yamauchi, N. Hirota, O. Kitao, and H. Nakatsuji, *Chem. Phys.* **107**, 81 (1986).

<sup>9</sup>(a) J. A. Menapace and E. R. Bernstein, *J. Phys. Chem.* (to be published);

(b) J. A. Menapace and E. R. Bernstein, *J. Phys. Chem.* (to be published).

<sup>10</sup>M. M. Carrabba, J. E. Kenny, W. R. Moomaw, J. Cordes, and M. Denton, *J. Phys. Chem.* **89**, 674 (1985).

<sup>11</sup>A. Hiraya, Y. Achiba, K. Kimura, and E. C. Lim, *J. Chem. Phys.* **81**, 3345 (1984).

<sup>12</sup>G. Nemethy, M. S. Pottle, and H. A. Scheraga, *J. Phys. Chem.* **87**, 1883 (1983).

<sup>13</sup>P. M. Felker and A. H. Zewail, *Chem. Phys. Lett.* **94**, 448 (1983).

<sup>14</sup>P. M. Felker and A. H. Zewail, *Chem. Phys. Lett.* **94**, 454 (1983).